Rev. Roum. Sci. Techn.– Électrotechn. et Énerg.
Vol. **70**, *1*, pp. 69–74, Bucarest, 2025

EXPERIMENTAL MEASUREMENTS IMPACT OF SWITCHING FREQUENCY FOR THE MOSFET CONTROL SIGNAL ON THE ELECTROMAGNETIC INTERFERENCES IN A SERIES CHOPPER

ABDELHAKIM ZEGHOUDI [1*], ABDELBER BENDAOUD[1], SEYF EDDINE BECHEKIR[1]

Keywords: Switching frequency; Electromagnetic interference; Serial chopper; Differential mode; Common mode.

Static converters consist of electronic switches, passive components (inductor, capacitor), and resistors, allowing the conversion of electrical energy from one form to another. However, the uses of semi-conductor components (MOSFET, IGBT, Thyristor, *etc*.) in switching are generating rapid variations of voltage (d*v*/d*t*) and current (d*i*/d*t*). This leads to high-frequency electromagnetic disturbances. This paper presents the study of electromagnetic disturbances conducted in common and differential modes in a series chopper by simulation using LTspice software. Experimental measurements validate the obtained results. Then, we studied the impact of variation of the switching frequency on the input current and the output voltage of the chopper, as well as on the disturbances conducted in two modes, common mode, and differential, by experimental measurements in the time and frequency domains. An Arduino program does these variations on the control signal parameters.

1. INTRODUCTION

The energy conversion in power electronics consists of two complementary phases: the switching by semiconductors and energy storage by passive components (capacitors and inductors) [1–6]. There are two types of switches: controlled switching (MOSFET, IGBT, thyristor, etc…) and others with uncontrolled switching (diodes).

Electronic switches are controlled by higher and higher frequencies, which generate swift variations of current and voltage as a function of time; this causes very constraining electromagnetic disturbances [7–11]. These disturbances are part of electromagnetic compatibility problems (EMC) in power electronics.

DC/DC converters are a relatively important part of the conversion chain. They are widely used in connections to storage batteries, photovoltaic systems, wind turbines, hybrid systems, and automotive applications [8,12].

This paper's main contribution is to study the impact of frequency variation on the switching of series choppers by experimental measurements of electromagnetic disturbances conducted in common and differential modes.

This paper is organized as follows: in section 2, the main factors of the switching cell that can affect the conducted electromagnetic disturbances are defined. Section 3 presents the serial chopper schema under LTspice software, and the results are extracted. The circuit is realized under PCB to validate the simulation results using the experimental measurements. In section 4, we study the impact of varying the switching frequency of the MOSFET on the conducted electromagnetic disturbances. by fixing the duty cycle at 50%. Variation: the Arduino program does the frequency. The experimental results are compiled and analyzed. In section 5, the conclusion is drawn from the simulation and experimental measurements results on the impact of variation of frequency of switching MOSFET in a series chopper**.**

2. SWITCHING CELL

The cell's switching properties are highly dependent on the characteristics of the load, the nature of the active switches used, and the type of control. Various factors specific to the switching cell can strongly affect the converter's spectral signature.

- ✓ Switching Time τ

The switching time is an essential factor in the disturbance generation mechanism because it controls the "d*v*/d*t*" and "d*i*/d*t*" [13-17], as shown in Fig. 1.

- ✓ Switching frequency F_s

The frequency of switching electronic switches is fundamental in energy conversion systems from one form to another [10–16].

- ✓ Parasitic components of the switching cell.

In the switching cell, parasitic elements such as wiring inductances, semiconductor self-capacitances, and capacitances between tracks and reference planes modify the converter's electrical functioning, creating repercussions on the spectrum [17–19].

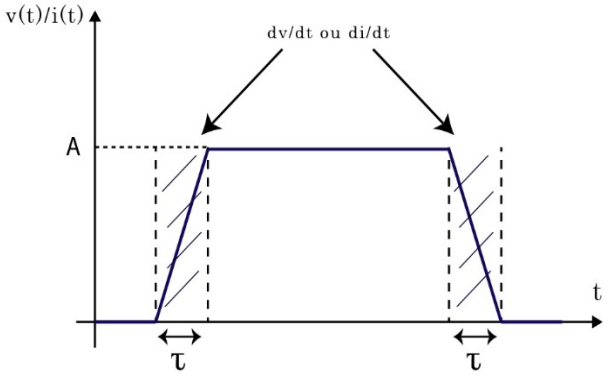

Fig. 1 – Trapezoidal waveform associated with switching [13].

3. INTRODUCTION

3.1 SIMULATION OF A BUCK CONVERTER

We simulated a buck converter under the LTspice software, as shown in Fig. 2. The main elements of the LTspice software circuit are the Line Impedance Stabilization Network "LISN," a 20 V DC source, another square source for controlling the MOSFET type IRF740, a diode of type MUR460, parasitic elements, and a resistor load of value 1.2 kΩ.

[1] APELEC Laboratory, Electrical Engineering Department, Djilali Liabes University, Sidi Bel Abbes, BP 22000, Algeria**.**
E-mail: abdelhakim.zeghoudi@univ-sba.dz, (Corresponding Author); abdelber.bendaoud@univ-sba.dz ; seyfeddine.bechekir@univ-sba.dz

DOI: 10.59277/RRST-EE.2025.1.12

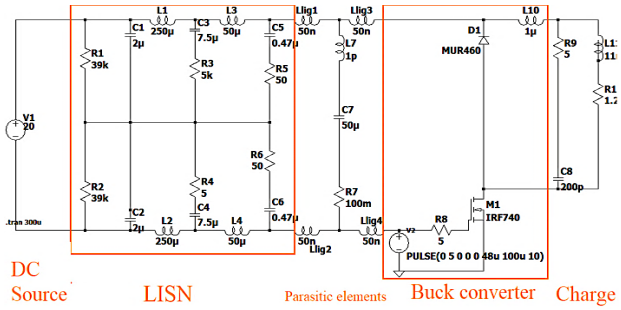

Fig. 2 – Serial chopper diagram with LISN realized by LTspice software

The MOSFET is controlled with a duty cycle of 50 % and a switching frequency of 10 kHz. The "LISN" device is connected to the start of the static converters to measure the conducted emissions in common mode and differential mode generated by this model

3.2 EXPERIMENTAL REALIZATION

The realization of the Buck static converter under a printed circuit board (PCB), as indicated in Fig. 3 is constituted of the following elements:

(1) Serial chopper input (+)
(2) serial chopper input (-)
(3) Arduino board input
(4) Regulator 12 V
(5) Regulator 15 V
(6) Capacitors 47 µF, 2.2 µF
(7) Driver IR2110
(8) Resistor 1 kΩ
(9) Diodes 1N4007
(10) MOSFET IRF740
(11) Chopper output (Resistance 1.2 k Ω)
(12) Power diode MUR460.

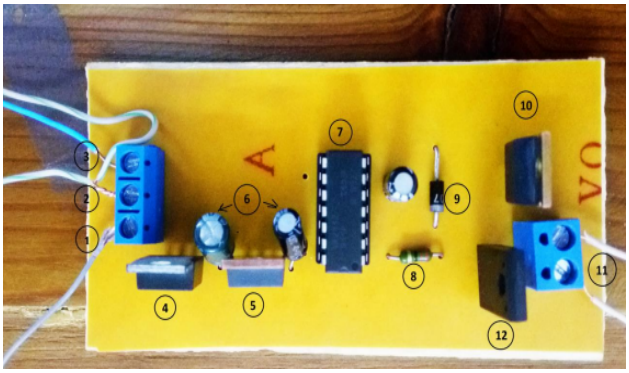

Fig. 3 – Printed circuit board of series chopper.

When the realization of the chopper was finished, we started to realize an experimental bench which is constituted by the following elements: a power supply in direct current 20 V to feed the chopper, an oscilloscope, a spectrum analyzer, and an amperometric probe for the measurement and the visualization of the electric magnitudes, and the electromagnetic disturbances in common and differential mode, a laptop and an Arduino card to generate the signal of command of the MOSFET of the static converter. The measurement bench realized in the APELEC laboratory is represented in Fig. 4.

Figure 5 presents a descriptive schema of the measurement bench of the conducted emissions generated by a chopper series.

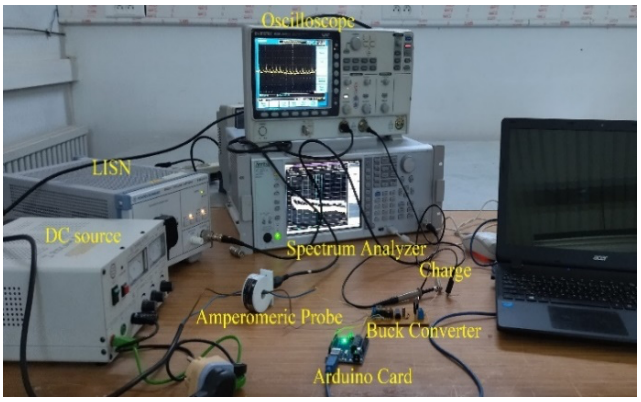

Fig. 4 – Photograph of the measurement bench of the electromagnetic disturbances generated by the buck converter.

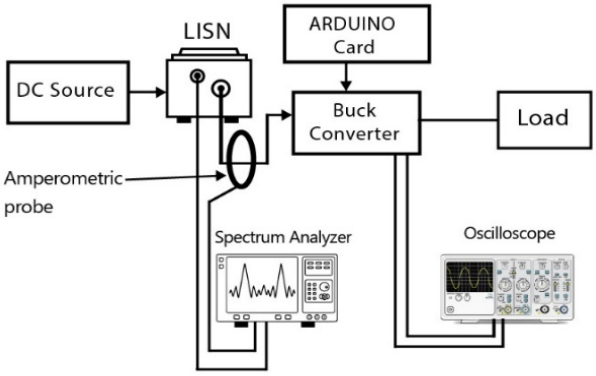

Fig. 5 – Descriptive diagram of the bench for measuring electromagnetic interference.

4. EMI MEASUREMENT

Figure 6 shows the temporal variation of the voltage across the load at the output of the converter. Where we notice a concordance between the simulation and the experimental results, we see that the voltage presents a square signal, which depends on the control signal of the MOSFET transistor with a duty cycle equal to 50 % of the switching frequency f = 10 kHz.

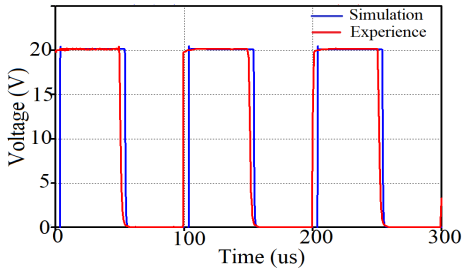

Fig. 6 – Temporal voltage response at the output of the series chopper.

4.1 COMMON MODE

In the common mode, the current flows in all conductors, and the ground returns in the same direction. Figure 7 shows the method of measuring the disturbances conducted in common mode by the amperometric probe [20–22].

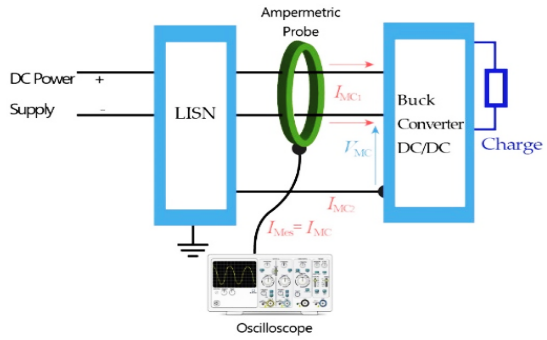

Fig. 7 – Descriptive diagram of electromagnetic disturbances in common mode.

Figures 8 and 9 show the time and frequency variation of the common mode current obtained by the simulation and experimental measurements. As shown in Figure 8, we notice a noise of about two mA with disturbance peaks.

In the frequency domain, Fig 9 shows an amplitude of width -90 dB to -180 dB in the range from 1 kHz to 100 MHz. We observe a slight disturbance between -90 dB and -140 dB in the frequency range from 1 kHz to 1 MHz.

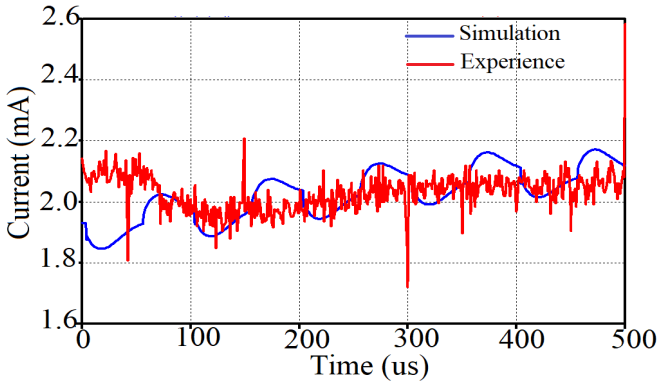

Fig. 8 – Temporal variation of the current in common mode.

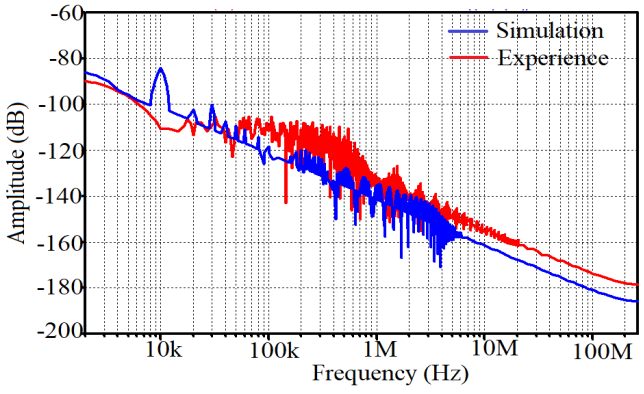

Fig. 9 – Frequency variation of the current in common mode.

4.2 DIFFERENTIAL MODE

In the differential mode, the current flows through a conductor to the victim and back through another conductor in the opposite direction, as shown in Fig.10, which presents the method of measuring the noise conducted in differential mode by the amperometric probe [20–22].

Figures 11 and 12 present the current in differential mode, respectively, in the time and frequency domains obtained by the simulation and the experimental measurements.

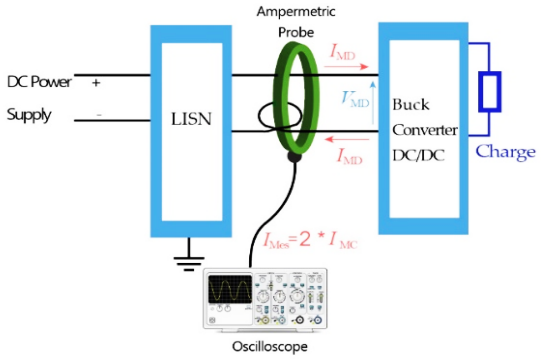

Fig. 10 – Descriptive diagram of electromagnetic disturbances in differential mode.

In Fig. 11, we notice the variation of the noises that depends on the MOSFET's switching frequency between -3 mA and 8 mA for the experimental results. In Fig. 12, for the frequency domain, we notice a gain of the disturbances of amplitude -50 dB for the switching frequency f = 10 kHz, then a minimization of the disturbances towards high frequencies.

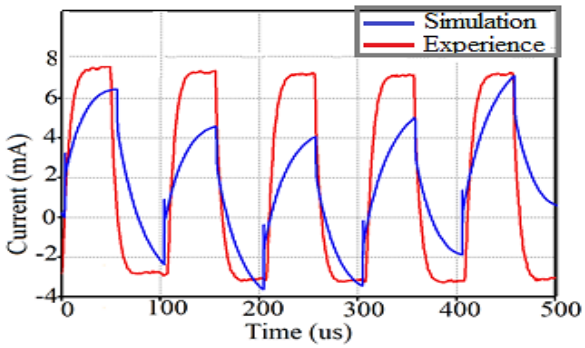

Fig. 11 – Temporal variation of the current in differential mode.

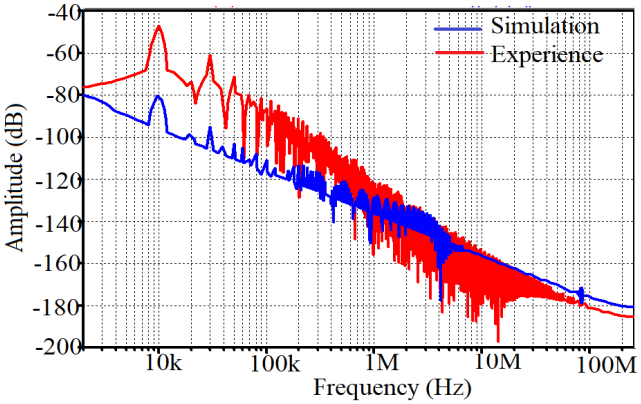

Fig. 12 – Differential mode current spectrum of a serial chopper.

5 IMPACTS OF VARYING THE SWITCHING FREQUENCY ON THE MOSFET

In this part, we are interested in measuring and visualizing the impact of variation of the parameters of control signal MOSFET in a serial chopper of square shape generated by the Arduino board on the noise in common mode and differential mode. Table 1 presents the switching frequencies that we have used in this work.

Table1

Frequencies generated by Arduino cards.

Frequency	Duty Cycles (%)	Time turn on (µs)	Time turn off (µs)
10 kHz	50	48	48
15 kHz	50	31	31
20.6 kHz	50	22	22
145.3 kHz	50	1	1

Figures 13 and 14 show the temporal and frequency response of the input current of the buck chopper as a function of the frequency variation. We have taken the following frequencies, f = 145.3 kHz, f = 20.6 kHz, and f = 15 kHz, by fixing the duty cycle at 50 %.

From the obtained results shown in Fig. 13, it is observed that with the increase of the control frequency, a very rapid oscillation of the current remains in a very low range of variation between 4 mA and 5 mA, as indicated in Fig. 13 by the green color, and the range of variation of the current increases with the reduction of the control frequency. However, in the frequency of f = 145.3 kHz, interesting peaks are observed due to the rapid variation of the current as a function of time. In the frequency domain shown in Fig. 14, it is consistent that the increase in frequency makes the disturbance peaks move away from high frequencies, but the noise in the range [145 kHz-100 MHz], which means that after the significant switching frequency of our test is still more important than other cases of frequencies: f = 15 kHz, f = 20.6 kHz and f = 145.3 kHz.

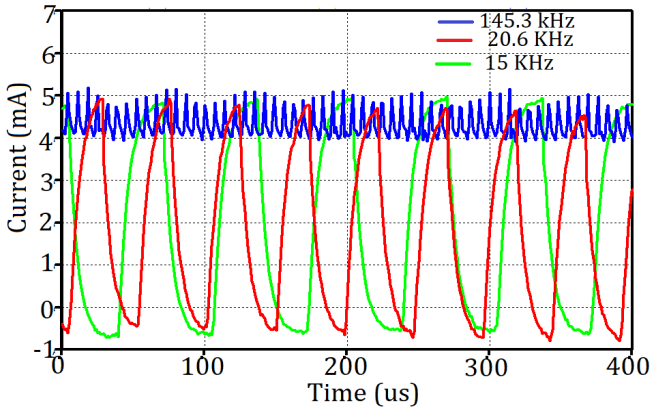

Fig. 13 – Temporal response of the input current as a function of the variation of the frequency of the MOSFET control signal generated by Arduino for duty cycle 50 %.

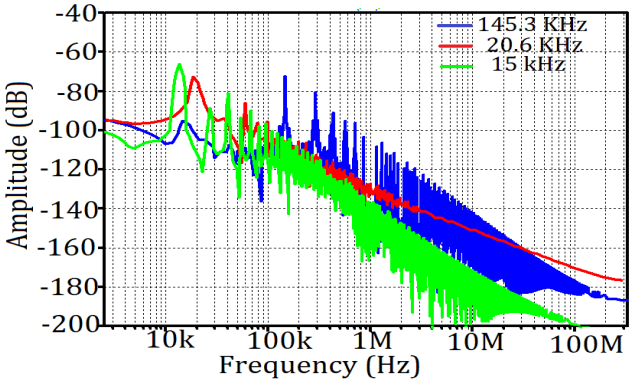

Fig. 14 – Frequency spectra of the input current as a function of the variation in the frequency of the MOSFET control signal generated by Arduino for duty cycle 50 %.

5.1 COMMON MODE SWITCHING FREQUENCY

Figures 15 and 16 show the electromagnetic disturbance of common mode currents in time and frequency domains as function of the variation of the switching frequency of the MOSFET, fixing the duty cycle at 50%.

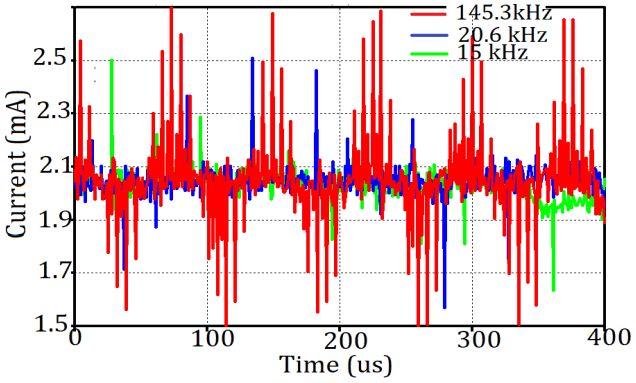

Fig. 15 – Temporal response of common mode current as a function of switching frequency variation of the MOSFET for a duty cycle of 50 %.

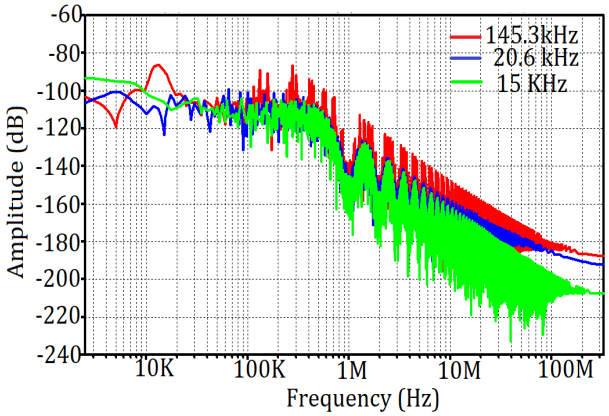

Fig. 16 – Frequency spectra of common mode current as a function of switching frequency of the MOSFET.

From the obtained results in Fig. 15, we notice that with the increase of the frequency, the oscillatory phenomenon increases with significant peaks compared to the fundamental frequencies, as indicated in Fig. 15. For Fig. 16 in the frequency domain, we observe the disturbances increases with the increase of the switching frequency with considerable gains in the range of frequency 100 kHz to 500 kHz, then minimization of disturbance for all the cases of towards the high frequencies.

5.2 DIFFERENTIAL MODE SWITCHING FREQUENCY

Figures 17 and 18 indicate the temporal and frequency response of the current disturbances in differential mode in the temporal and frequency domains for various frequencies by fixing the duty cycle at 50 %. We notice an oscillatory phenomenon in the temporal domain with current peaks for the frequency f = 145.3 kHz. This phenomenon can be explained by the fast variation of switching the MOSFET, which causes a variation of voltage and current very fast according to time. For Fig. 18, which presents the frequency domain, one notices a gain of amplitude -60 dB for the frequency of approximately 20 kHz. With the increased frequency of switching the MOSFET, for example, f = 145. 3 kHz, we also observe an amplitude gain of -70 dB at the switching frequency. So, we observe the conducted disturbances in the first range between [1 kHz - 145.3 kHz] essential in the case of the frequency is low; after the large switching frequency, the noise in this last frequency becomes very important, as indicated in Fig. 18 with f = 145.3 kHz.

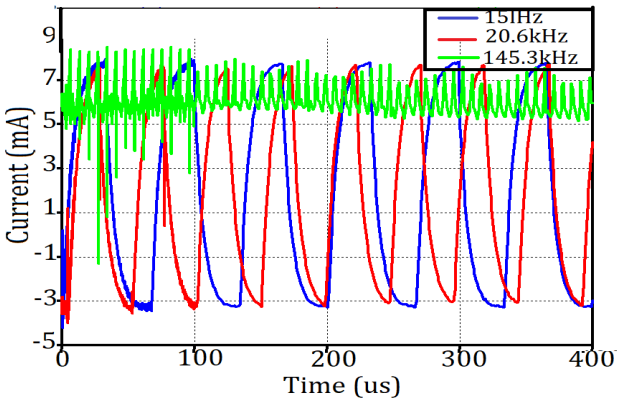

Fig. 17 – Temporal response of the current in differential mode as a function of the switching frequency variation of the MOSFET for a duty cycle of 50 %.

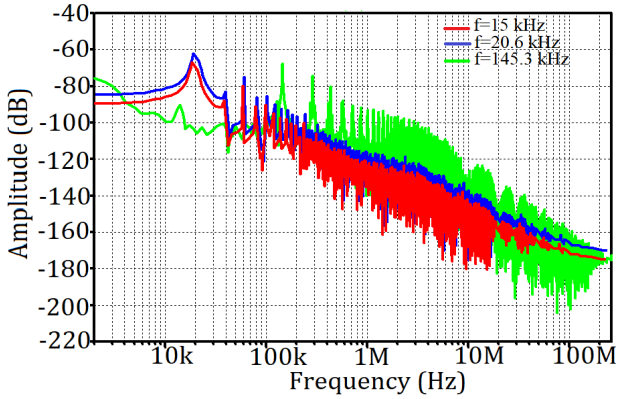

Fig. 18 – Frequency spectra of the current in differential mode as a function of the switching frequency of the MOSFET.

6. CONCLUSION

This paper presents a comparative study of the impact of varying the switching frequency of the MOSFET by fixing the duty cycle at 50 % in the time and frequency domains to measure the electromagnetic disturbances in common mode and differential mode.

First, we started by studying a serial chopper under LTspice software, then with experimental measurements on the serial chopper realized in the laboratory to validate the obtained results. Then, we varied the switching frequency of control the MOSFET by the Arduino program: $f = 10$ kHz, $f = 15$ kHz, $f = 20.6$ kHz, and $f = 145.3$ kHz, and finally measured the conducted electromagnetic disturbances in two modes.

It is concluded that the conducted disturbance in differential mode is much more significant than the common mode, as well as the increase of the frequency has two different points: before the switching frequency, the disturbances are less intense, and after the switching frequency, the disturbances are increased with essential peaks. For this case, the increase of frequency in the electronic systems plays the role of the system speed and distancing the disturbances towards the high frequencies; therefore, it is necessary to choose well the frequency of control of the MOSFET that depends on the electrical systems that we use, concerning the requirement of the EMC standard.

ACKNOWLEDG(E)MENT(S)

The authors of APELEC Laboratory, Djillali Liabès University of Sidi Bel-Abbès, would also like to thank the General Directorate of Scientific Research and Technological Development (DGRSDT) in Algeria for their technical support and the specific research budget allocated to this program.

CREDIT AUTHORSHIP CONTRIBUTION STATEMENT

Abdelhakim Zeghoudi contributed significantly to the study's conception and design, particularly in defining the experimental framework and methodology for studying electromagnetic disturbances in the serial chopper. They also played a key role in the simulation work using LTspice software, ensuring accurate modeling and analysis of the converter's behavior.

Abdelber Bendaoud was involved in the mechanical and technical aspects of the experimental setup, including the design and realization of the printed circuit board (PCB) for the buck converter. He participated in the experimental measurements and contributed to the final revision and structuring of the paper.

Seyf Eddine Bechekir was responsible for the experimental setup. Using the Arduino program, they implemented the control signal and performed the necessary measurements and data acquisition.

Received on 27 April 2024

REFERENCES

1. A.G. Aulagnier, M.C. Cousineau, T.M. Meynard, E. Rolland, K. Abouda. *High frequency EMC impact of switching to improve DC-DC converter performances*. European Conference on Power Electronics and Applications, pp. 1–9 (2013).
2. K. Muttaqui, M. Haque. *Electromagnetic interference generated from fast switching power electronic devices*. International Journal of Innovations in Energy Systems and Power, **3**, *1*, pp. 19–45 (2018).
3. A.A. Ales, A. Gouichiche, Z. Karouche, B. Moussaoui, D. Sachen, J.L. Roudet. *The accurate input impedances of a DC/DC converters connected to the network*. IEEE International Conference on Environment and Electrical Engineering, pp. 1–6 (2005).
4. H. Slimani, A. Zeghoudi, A. Bendaoud, A. Reguig, B. Benazza, N. Benhadda. *Experimental measurement of conducted emissions generated by static converters in common and differential modes*. European Journal of Electrical Engineering (EJEE), **23**, *3*, pp. 273–279 (2021).
5. A. Zeghoudi, A. Bendaoud, H. Slimani, B. Benazza, J. Bennouna. *Determination of electromagnetic disturbances in a buck chopper*. Australian Journal of Electrical and Electronics Engineering (2022).
6. A. Zeghoudi, H. Slimani, A. Bendaoud, A. Benazza, S. Bechekir, H. Miloudi. *Measurement and analysis of common and differential modes conducted emissions generated by an AC/DC converter*. Electrical Engineering & Electromechanics, **1**, pp. 3–9 (2022).
7. B. Benazza, A. Bendaoud, J.L. Schanen. *Etude exprimentale sur l'impact des emissions CEM du au positionement d'un convertisseur statique DC-DC entre une source et une charge*. Colloque International et Exposition sur la Compatibilite Electromagnetique (CEM), pp. 1–6 (2018).
8. A. Zeghoudi, A. Bendaoud, H. Slimani, H. Miloudi, M. Miloudi, N. Chikhi. *Experimental measurement of common and differential modes for variable speed drive DC motor*. IEEE Multiconference on Signal, Systems, Devices, Setif, Algeria (2022).
9. O. Laudatu, D. Niculae, M.I. Iordache, M.-L. Bobaru, M. Stanculescu. *Experimental analysis of power semiconductor elements used in flyback converters*. Rev. Roum. Sci. Techn.– Electrotechn. Et Energ., **69**, *1*, pp. 67–72 (2024).
10. A.A. Saafan, V. Khadkikar, M.S.E. Moursi, H.H. Zeineldin. *A new multiport DC-DC converter for DC microgrid applications*. IEEE Transactions on Industry Applications, **59**, *1*, pp. 601-611 (2023).
11. S. Latreche, B. Babes, A. Bouafassa. *Design and real-time implementation of synergetic regulator for a DC-DC boost converter*. Rev. Roum. Sci. Techn.– Electrotechn. Et Energ., **69**, *3*, pp. 305–310 (2024).
12. B. Khvitia, A. Gheonjian, Z. Kutchadze, R. Jobava. *A SPICE model for IGBTs and power MOSFETs focusing on EMI/EMC in high-voltage systems*. Electronics, **10**, pp. 2822 (2021).
13. L. Han, L. Liang, Y. Wang, X. Tang, S. Bai. *Performance limits of high voltage press-pack SiC IGBT and SiC MOSFET devices*. Power Electronic Devices and Components, **3**, 100019 (2022).
14. A. Zeghoudi, A. Bendaoud, L. Canale, A. Tilmatine, H. Slimani.

Common mode and differential mode noise of AC/DC LED driver. IEEE International Conference on Environment and Electrical Engineering and IEEE Industrial and Commercial Power Systems Europe, pp. 1–6 (2021).
15. S. Bechekir, A. Zeghoudi, D. Ould-Abdeslam, M. Brahami, H. Slimani, A. Bendaoud. *Development of a boost-inverter converter under electromagnetic compatibility stress equipping a photovoltaic generator*. Electrical Engineering & Electromechanics, **5**, pp. 14–19 (2023).
16. G. Angenieux. *Transmission lines in harmonic and transient regime*. University of Savoy, France (2009).
17. M.I. Montrose. *Printed circuit board design techniques for EMC compliance – A handbook for designers*, Second Edition. New York: John Wiley & Sons, Inc. (2000).
18. Y. Zhang, S. Wang. *Characterization and design of filter inductors and capacitors to suppress the radiated EMI in a power converter*. International Power Electronics Conference (IPEC-Himeji ECCE Asia), Himeji, Japan, pp. 1082–1089 (2022).
19. M. Miloudi, A. Bendaoud, H. Miloudi, S. Nemmich. *Etude et réduction des emissions conduite générées par une alimentation à découpage*. Proc. Int. Conf. CI'03, Tizi–Ouzou, Algérie, April (2013).
20. B. Revol. *Applied EMC in power electronics*, Ecole normale supérieure Scalard-Paris (12/03/2018).
21. A. Zeghoudi, H. Slimani, A. Bendaoud, B. Benazza, H. Miloudi, L. Canale. *Power impact and electromagnetic disturbances of different lighting modes from spot LED lamp*. Optik - International Journal of Light and Electron Optics (2022).
22. A. Zeghoudi, A. Bendaoud, S. Khalladi, S. Slimani, H. Miloudi, L. Canale. *Common and differential modes filter for the PFC boost AC/DC LED driver*. 22nd International Conference on Environment and Electrical Engineering, 6th Industrial and Commercial Power Systems Europe, Prague, Czech Republic, June 28th - July 1st (2022).